ORIGINAL RESEARCH

Cigarette Smoke–Induced Disruption of Bronchial Epithelial Tight Junctions Is Prevented by Transforming Growth Factor-β

Andrea C. Schamberger, Nikica Mise, Jie Jia, Emmanuelle Genoyer, Ali Ö. Yildirim, Silke Meiners, and Oliver Eickelberg

Comprehensive Pneumology Center, Institute of Lung Biology and Disease, University Hospital, Ludwig-Maximilians-University and Helmholtz Zentrum München, Member of the German Center for Lung Research, Munich, Germany

Abstract

The airway epithelium constitutes an essential immunological and cytoprotective barrier to inhaled insults, such as cigarette smoke, environmental particles, or viruses. Although bronchial epithelial integrity is crucial for airway homeostasis, defective epithelial barrier function contributes to chronic obstructive pulmonary disease (COPD). Tight junctions at the apical side of epithelial cell–cell contacts determine epithelial permeability. Cigarette smoke exposure, the major risk factor for COPD, is suggested to impair tight junction integrity; however, detailed mechanisms thereof remain elusive. We investigated whether cigarette smoke extract (CSE) and transforming growth factor (TGF)-β1 affected tight junction integrity. Exposure of human bronchial epithelial cells (16HBE14o$^-$) and differentiated primary human bronchial epithelial cells (pHBECs) to CSE significantly disrupted tight junction integrity and barrier function. Specifically, CSE decreased transepithelial electrical resistance (TEER) and tight junction–associated protein levels. Zonula occludens (ZO)-1 and ZO-2 protein levels were significantly reduced and dislocated from the cell membrane, as observed by fractionation and immunofluorescence analysis. These findings were reproduced in isolated bronchi exposed to CSE *ex vivo*, as detected by real-time quantitative reverse-transcriptase PCR and immunohistochemistry. Combined treatment of 16HBE14o$^-$ cells or pHBECs with CSE and TGF-β1 restored ZO-1 and ZO-2 levels. TGF-β1 cotreatment restored membrane localization of ZO-1 and ZO-2 protein and prevented CSE-mediated TEER decrease. In conclusion, CSE led to the disruption of tight junctions of human bronchial epithelial cells, and TGF-β1 counteracted this CSE-induced effect. Thus, TGF-β1 may serve as a protective factor for bronchial epithelial cell homeostasis in diseases such as COPD.

Keywords: zonula occludens; airway epithelium; chronic obstructive pulmonary disease; ciliated cell

Clinical Relevance

Cigarette smoking is the major risk factor for chronic obstructive pulmonary disease (COPD). Here we show that cigarette smoke extract (CSE) led to the disruption of tight junctions of human bronchial epithelial cells and that transforming growth factor (TGF)-β1 counteracted this CSE-induced effect. Thus, TGF-β1 may serve as a protective factor for bronchial epithelial cell homeostasis in diseases such as COPD.

Chronic obstructive pulmonary disease (COPD), the fourth leading cause of death worldwide (1), is induced by environmental exposure to noxious gases, particles, indoor fumes, pathogens, or, most importantly, by active or passive exposure to cigarette smoke (2). COPD is characterized by progressive airflow limitation due to an abnormal inflammatory response and structural pathological remodeling of the lung to these environmental exposures (3). The airway epithelium represents the lung's first line of defense; therefore, its barrier function and integrity is tightly regulated to prevent epithelial and interstitial damage (4). Cigarette smoke exposure leads to damage and increased permeability of the airway epithelium, as recently demonstrated *in vitro* in human bronchial epithelial cells (HBECs) (5) and in patients with COPD compared with nonsmokers

(Received in original form February 27, 2013; accepted in final form December 15, 2013)

This work was supported by the Helmholtz Association and by a RISE fellowship from the German Academic Exchange Service (DAAD, PKZ: A/12/07058) (E.G.).

Correspondence and requests for reprints should be addressed to Oliver Eickelberg, M.D., Comprehensive Pneumology Center, Ludwig-Maximilians-Universität and Helmholtz Zentrum München, Max-Lebsche-Platz 31, 81377 München, Germany. E-mail: oliver.eickelberg@helmholtz-muenchen.de

This article has an online supplement, which is accessible from this issue's table of contents at www.atsjournals.org

Am J Respir Cell Mol Biol Vol 50, Iss 6, pp 1040–1052, Jun 2014

Originally Published in Press as DOI: 10.1165/rcmb.2013-0090OC on December 20, 2013
Internet address: www.atsjournals.org

and smokers (6). Animal studies using tracer molecules have shown that the epithelial permeability increases after smoke exposure (7, 8). These changes in permeability were transient and reversible (9). As such, we sought to elucidate the mechanisms of epithelial permeability, particularly tight junction disassembly, in response to cigarette smoke exposure in the bronchial epithelium.

Tight junctions are located at the most apical side of epithelial cell–cell contacts and represent the major junctional components determining the permeability of an epithelial sheet. Tight junctions are critically involved in the exchange of ions, solutes, and cells that travel across paracellular spaces. Furthermore, tight junctions regulate the formation of apico-basal polarity and control proliferation, gene expression, or cell differentiation through signaling pathways that are activated by tight junction components (10). More than 40 different proteins have been identified to be associated with tight junctions (11): occludin (OCLN) and claudins (CLDs), for example, are transmembrane spanning proteins forming the intercellular adhesions via hemophilic and heterophilic interactions. Zonula occludens (ZO)-1, ZO-2, ZO-3, cingulin, and MAGI1 are located intracellularly and anchor transmembrane proteins with the actin cytoskeleton (10).

Cigarette smoke contains a complex mixture of approximately 4,800 chemicals (12), making it difficult to define the cellular mechanisms that lead to smoking-related features of COPD in general and of injury of the airway epithelium in particular. A recent study demonstrated a transient decrease in airway epithelial barrier function in bronchial epithelial cells (13). In addition, human adenocarcinoma Calu-3 cells exposed to mainstream smoke exhibited decreased transepithelial electrical resistance (TEER), resulting from a highly regulated yet undefined process not due to the cytotoxicity of cigarette smoke (14). Down-regulation of apical tight junction components, including CLDs, was observed in chronic exposures of bronchial epithelial cells to cigarette smoke extract (CSE) (15, 16).

The multifunctional cytokine transforming growth factor (TGF)-β exhibits immunosuppressive capacity and is produced by virtually all cell types in the lung (17). TGF-β receptor activation leads to phosphorylation of Smad2/3, complex formation with Smad4, and translocation to the nucleus, in turn regulating transcriptional activation and/or repression of selected target genes. Smad-dependent signaling can be inhibited by Smad6 or -7, both inhibitory Smad isoforms that are activated by, for example, IFN-γ or TNF-α stimulation. TGF-β is thought to significantly contribute to the pathogenesis of COPD (18), but its pleiotropic actions make it difficult to assign distinct cellular functions during disease pathogenesis. For instance, smokers or ex-smokers with COPD revealed augmented TGF-β1 expression levels in bronchiolar epithelial cells (19). In contrast, a single nucleotide polymorphism within the first exon of the TGF-β gene (reference ID: 1,982,073), which is associated with increased TGF-β levels, is more frequent in control and smoke-resistant subjects than in patients with COPD, suggesting that TGF-β could also have a protective role in COPD (20). In accordance with this notion, studies of intestinal epithelial cells have recently shown that TGF-β is also able to rescue epithelial barrier function (21–25). Although TEER is increased in colon-derived epithelial cells treated with TGF-β (22, 23, 25), disruption of the intestinal epithelial barrier is counteracted by TGF-β (21–24). In addition, TGF-β blocked *Escherichia coli*–induced increased permeability via maintenance of CLD-2, OCLN, and ZO-1 levels in intestinal epithelial cells (25), highly suggesting cell-specific effects of TGF-β function on epithelial integrity.

Accordingly, we hypothesized that TGF-β exerted protective functions on the bronchial epithelium exposed to cigarette smoke. To this end, we characterized the regulation and function of tight junctions and the role of TGF-β in response to cigarette smoke–induced epithelial barrier dysfunction. Our data demonstrate that bronchial epithelial barrier function was impaired due to tight junction disintegration when exposed to nontoxic doses of CSE and that TGF-β was able to prevent these changes. Understanding these mechanisms in greater detail will facilitate controlled regeneration of dysfunctional epithelial permeability to restore lung epithelial barrier function and integrity in diseases such as COPD.

Materials and Methods

Cells Culture and Treatment

The 16HBE14o$^-$ HBEC line was cultured in MEM (PAA-Laboratories, Pasching, Austria) supplemented with 10% FBS. If not stated otherwise, cells were seeded at a density of 2×10^4 cells/cm^2 and treated 48 hours later. CSE and/or TGF-β1 (R&D, Minneapolis, MN) treatment was performed every 24 hours. Chronic treatment was performed as shown in Figure E4A in the online supplement. Normal primary HBECs (pHBECs) (Lonza, Wokingham, UK) were expanded in BEGM media (Lonza). Cells were seeded at passage 2 or 3 at a density of 1×10^4 cells/cm^2 and treated when confluent. For differentiation, cells were seeded at passage 2 at a density of 1×10^5 cells/cm^2 on human placental collagen type IV–coated (Sigma-Aldrich, St. Louis, MO) transwell inserts (transparent, 0.4 μm; Greiner, Solingen, Germany) in BEGM media. Cells were lifted to the air–liquid interface (ALI) when confluent, apical media was aspirated, and basolateral media was substituted with PneumaCult-ALI media (Stemcell Technologies, Köln, Germany) and changed every other day. If not stated otherwise, cells were treated at Day 14 after air-lift with CSE (apical, 80 μl) and/or TGF-β1 (apical and basolateral). The extent of differentiation was quantified using Imaris 7.4.0 software (Bitplane, Zurich, Switzerland). Z-stack images of stained cultures were obtained by confocal microscopy (LSM710 System; Carl Zeiss, Oberkochen, Germany), and 1,500 to 3,500 cells per image were analyzed for positivity of differentiation makers. Ten images per group and time point were processed.

Preparation of CSE

CSE (100%) was generated as previously described (26). Further details are provided in the online supplement.

Cytotoxicity Assays

Details are provided in the online supplement.

TEER Measurements

For 16HBE14o$^-$ cells, 1×10^5 cells/cm^2 were seeded onto rat-tail collagen type I or human-placental collagen type IV (Sigma-Aldrich)-coated (10 μg/cm^2) 12-well transwell inserts (transparent, 0.4 μm; Greiner) with 500 μl apical and 1,500 μl basolateral volumes.

Table 1: Primer Used for Real-Time Quantitative Reverse-Transcriptase Real-Time Polymerase Chain Reaction

Gene	Forward Primer (5′–3′)	Reverse Primer (5′–3′)
human CDH1	AACAGGATGGCTGAAGGTGACAGA	AACTGCATTCCCGTTGGATGACAC
human CLD4	TCCTGACTCACGGTGCAAAG	CGTAGGATTCCAAGCGCTG
human CLD6	TGCAGCTCCTTCAACCTCG	GTGTCAGGACGACTCCCAGG
human CYP1A1	ATGGTCAGAGCATGTCCTTCAGC	TGGGTCAGAGGCAATGGAGAAACT
human FN1	CCGACCAGAAGTTTGGGTTCT	CAATGCGGTACATGACCCCT
human HPRT	AAGGACCCCACGAAGTGTTG	GGCTTTGTATTTTGCTTTTCCA
human OCLN	AACCCAACTGCTCAGTCTTC	TGATCCACGTAGAGTCCAGTAG
human SNAI1/SNAIL	TGTCAGATGAGGACAGTGGGAA	GCCTCCAAGGAAGAGACTGAAGTA
human ZO-1	CAGCCGGTCACGATCTCCT	TCCGGAGACTGCCATTGC
human ZO-2	TTGAAGACACGGACGGTGAA	GTGATGGACGACACCAGCG
mouse HPRT	CCTAAGATGAGCGCAAGTTGAA	CCACAGGACTAGAACACCTGCTAAT
mouse ZO-1	CAGCCGGTCACGATCTCCT	CCGGAGACTGCCATTGC

Definition of abbreviations: CDH1, E-cadherin; CLD, claudin; CYP1A1, cytochrome P450-1A1; FN1, fibronectin 1; HPRT, hypoxanthine-guanine phosphoribosyltransferase; OCLN, occludin; SNAI1/SNAIL, SNAIL homolog 1; ZO, zonula occludens.

TEER was monitored using a Millicell-ERS-2 (Millipore, Billerica, MA) volt-ohm meter. Cells were treated at the indicated time points with CSE (apical) and/or TGF-β1 (apical and basolateral), and TEER was assessed at the indicated time points. For TEER assessment in differentiated pHBECs, 500 μl BEGM media was added to the apical compartment.

Cell Fractionation and Western Blot Analysis

Details are provided in the online supplement.

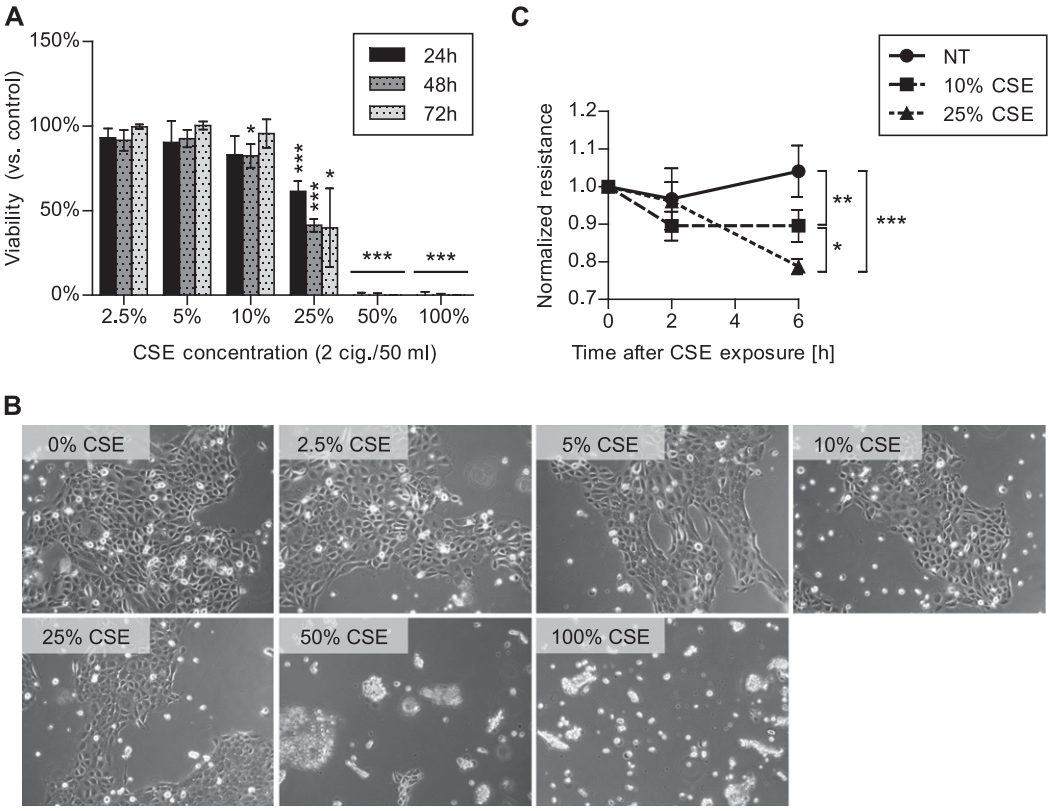

Figure 1. Cigarette smoke extract (CSE) affects cell viability and epithelial resistance of 16HBE14o$^-$ cells. (*A*) MTT assay of subconfluent 16HBE14o$^-$ cells treated every 24 hours with 0 to 100% CSE for up to 72 hours. Data were normalized to time-matched controls and represent mean ± SD of three independent experiments. For statistical analysis, Student's *t* test was used versus control. (*B*) Cell morphology of 16HBE14o$^-$ cells treated with indicated concentrations of CSE for 24 hours. Representative bright field images are shown (original magnification: ×100). (*C*) Analysis of transepithelial electrical resistance (TEER) from 16HBE14o$^-$ cells after exposure to 0 (nontreated [NT]), 10, or 25% CSE for up to 6 hours. Data were normalized to pretreatment TEER values (518 ± 56 Ω) and represent mean ± SD of four independent experiments. For statistical analysis, one-way ANOVA was used. For all experiments, $^*P < 0.05$, $^{**}P < 0.01$, and $^{***}P < 0.001$.

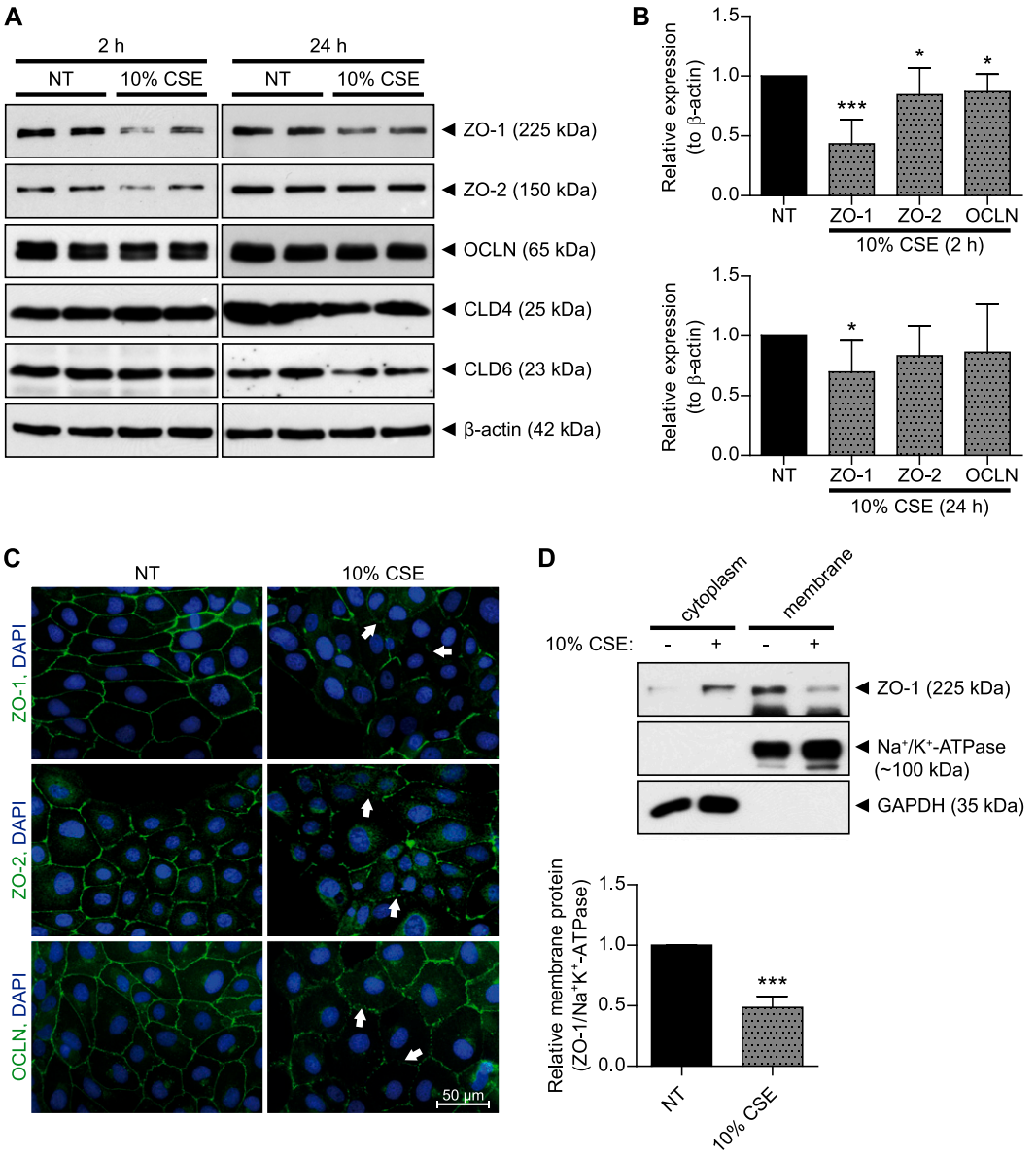

Figure 2. Short-term exposure to CSE disrupts tight junctions in 16HBE14o$^-$ cells. (*A*) Western blot analysis of protein extracts from 16HBE14o$^-$ NT cells or cells treated with 10% CSE for 2 and 24 hours. Representative blots of different tight junction proteins with representative β-actin as a loading control are shown. Duplicates of each condition were loaded onto the gels. (*B*) Protein levels were quantified. Data are depicted as mean ± SD of independent experiments relative to β-actin (n = 11–15 [2 h] and n = 6–9 [24 h]). Student's t test versus NT: $^*P < 0.05$, $^{**}P < 0.01$, and $^{***}P < 0.001$. (*C*) Indirect immunofluorescence analysis of 16HBE14o$^-$ cells NT or treated with 10% CSE for 72 hours (treatment every 24 h). Representative ZO-1, ZO-2, and OCLN staining is shown in *green*, and 4',6-diamidino-2-phenylindole (DAPI) staining is shown in *blue*. *Scale bar*: 50 μm. *White arrows* indicate disrupted tight junctions between the cells on CSE exposure. (*D*) Cells were NT or treated with 10% CSE for 2 hours, and cytoplasmic and membrane proteins were fractionated and analyzed via Western blot analysis. Na^+/K^+-ATPase and glyceraldehyde 3-phosphate dehydrogenase (GAPDH) represent markers for membrane and cytoplasmic fractions, respectively. Representative blots are shown, and densitometry analysis of membrane-bound ZO-1 was performed using Image Lab software. Data are depicted as mean ± SD of three independent experiments relative to Na^+/K^+-ATPase. $^{***}P < 0.001$ (Student's t test versus NT). CLD, claudin; OCLN, occludin; ZO, zonula occludens.

Cigarette Smoke Exposure of Isolated Airways

Airways were isolated from healthy female C57BL/6 mice (Charles River Laboratories, Sulzfeld, Germany) (27), washed, and incubated in CSE (six samples each) for 2 hours on 6-well transwell inserts (Greiner). Apical media was transferred to the basal compartment, and airways were cultured at the ALI for an additional 4 or 22 hours. For analysis, airways were embedded twice with 2% agarose medium and once with paraffin for immunohistochemistry or frozen in liquid nitrogen for subsequent RNA isolation.

RNA Isolation and Real-Time Quantitative Reverse-Transcriptase PCR Analysis

For specific gene amplification, primers listed in Table 1 were used. Further details are provided in the online supplement.

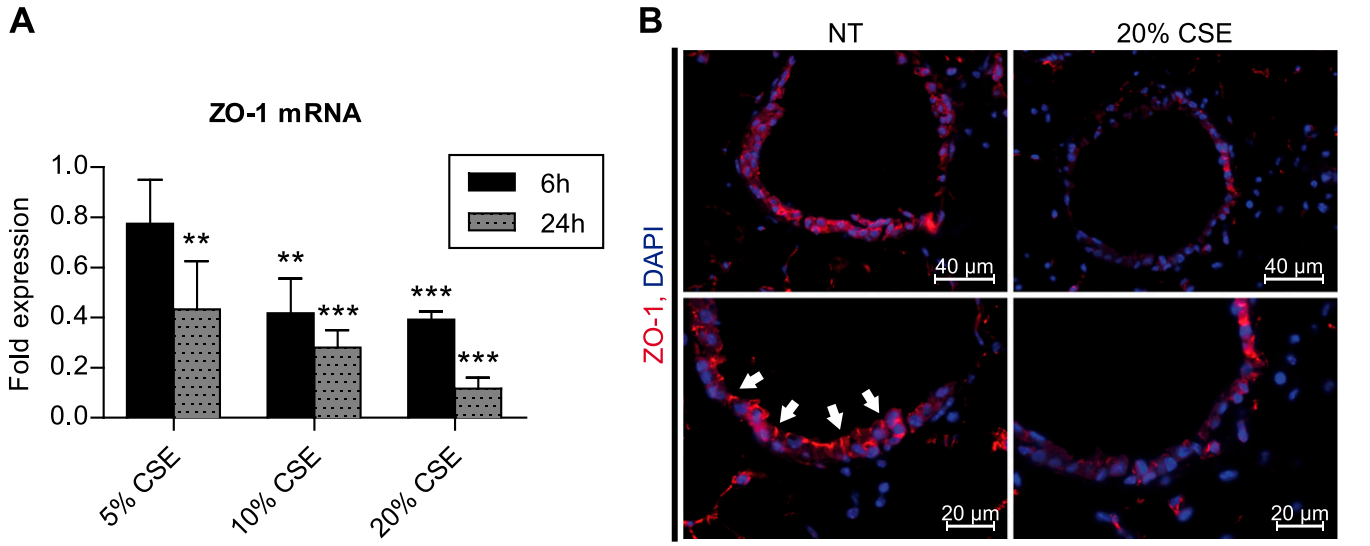

Figure 3. ZO-1 is down-regulated in smoke exposed bronchi from mice. (*A*) real-time quantitative reverse-transcriptase PCR analysis of expression levels of ZO-1 mRNA. Mouse bronchi were treated *ex vivo* with 5, 10, or 20% CSE for 6 and 24 hours, and values depict mean ± SD relative to time-matched controls (n = 3 per group). *$P < 0.05$; **$P < 0.01$; ***$P < 0.001$ (Student's t test vs. controls). (*B*) Paraffin sections from control (NT) and smoke-exposed bronchi for 24 hours are shown in two different magnifications. *Scale bars* = 40 μm (*upper panel*) and 20 μm (*lower panel*). Representative ZO-1 immunostaining is shown in *red*, and DAPI staining is shown in *blue*. *White arrows* indicate intact tight junctions in control bronchi.

Immunofluorescence and Immunohistochemistry Analysis

Immunostaining of cells (28) and paraffin sections (3 μm) (29) were performed as described previously.

Results

CSE Decreases Barrier Function in Bronchial Epithelial Cells

To identify nontoxic doses of CSE, we treated normal human bronchial epithelial 16HBE14o$^-$ cells with a range of CSE concentrations for 24, 48, or 72 hours and assessed cell viability by MTT assay (Figure 1A). As shown, 10% CSE was well tolerated by bronchial cells for up to 3 days of exposure. In contrast, 25% CSE significantly reduced cell viability after 24 hours, which was further exacerbated with prolonged CSE treatment. Importantly, 50 and 100% CSE induced pronounced cell death as early as 24 hours after exposure. Similar results were obtained by FACS analysis using PI/Annexin V staining (Figure E3B). 16HBE14o$^-$ cell morphology was not significantly changed after 24 hours of CSE stimulation using nontoxic doses (Figure 1B). Sensitivity of 16HBE14o$^-$ cells to CSE was strongly dependent on cell confluence. Exposure to 25% CSE had no influence on cell viability in confluent cultures (Figure E1). Exposure of bronchial epithelial cells to 10% CSE for 6 hours significantly decreased TEER compared with control (nontreated [NT]) conditions (Figure 1C). This effect was enhanced using 25% CSE. These data demonstrate that CSE specifically impairs barrier function *in vitro* in normal bronchial epithelial cells as early as 6 hours after exposure to nontoxic doses of CSE.

CSE-Induced Barrier Dysfunction Involves Down-Regulation of Tight Junction Molecules

To elucidate the mechanisms of CSE-induced barrier dysfunction, we investigated the expression and localization of cell–cell adhesion components. Bronchial epithelial cells were exposed for 2 or 24 hours to 10% CSE, and levels of the tight junction molecules ZO-1, ZO-2, OCLN, CLD-4, and CLD-6 were analyzed by Western blot analysis (Figures 2A and 2B). CSE exposure significantly diminished ZO-1 protein levels within 2 hours. Protein levels of ZO-2 and OCLN were significantly reduced after 2 hours, albeit to a lesser extent, but fully recovered within 24 hours. In contrast, decreased protein levels of CLD-4 and CLD-6 were observed after 24 hours of CSE injury. The mRNA levels of tight junction proteins did not change within 24 hours of CSE treatment (Figure E2), indicating posttranscriptional or posttranslational regulation of tight junction proteins in response to CSE. To further investigate this issue, we performed immunofluorescence staining for ZO-1, ZO-2, or OCLN of 16HBE14o$^-$ cells treated with or without 10% CSE for 72 hours (Figure 2C). Control cells demonstrated continuous membrane localization of ZO-1 expression. Additional fractionation analysis (Figure 2D) confirmed that ZO-1 protein was mainly present in the membrane fraction of unstimulated cells. On CSE exposure, continuous staining of ZO-1 was disrupted and appeared as discontinuous and fragmented, demonstrating disruption of tight junctions (Figure 2C). In accordance with this observation, ZO-1 protein decreased in the membrane fraction as early as 2 hours after CSE treatment and was detected in the cytoplasmic fraction (Figure 2D). Membrane-associated ZO-1 protein levels were significantly diminished by approximately 50% within this time period, as quantified by densitometry analysis using Na^+/K^+-ATPase as a membrane marker. Furthermore, staining for ZO-2 and OCLN (Figure 2C) resembled the staining of ZO-1 in control and in CSE-exposed cells. Taken together, these results indicate that tight junction

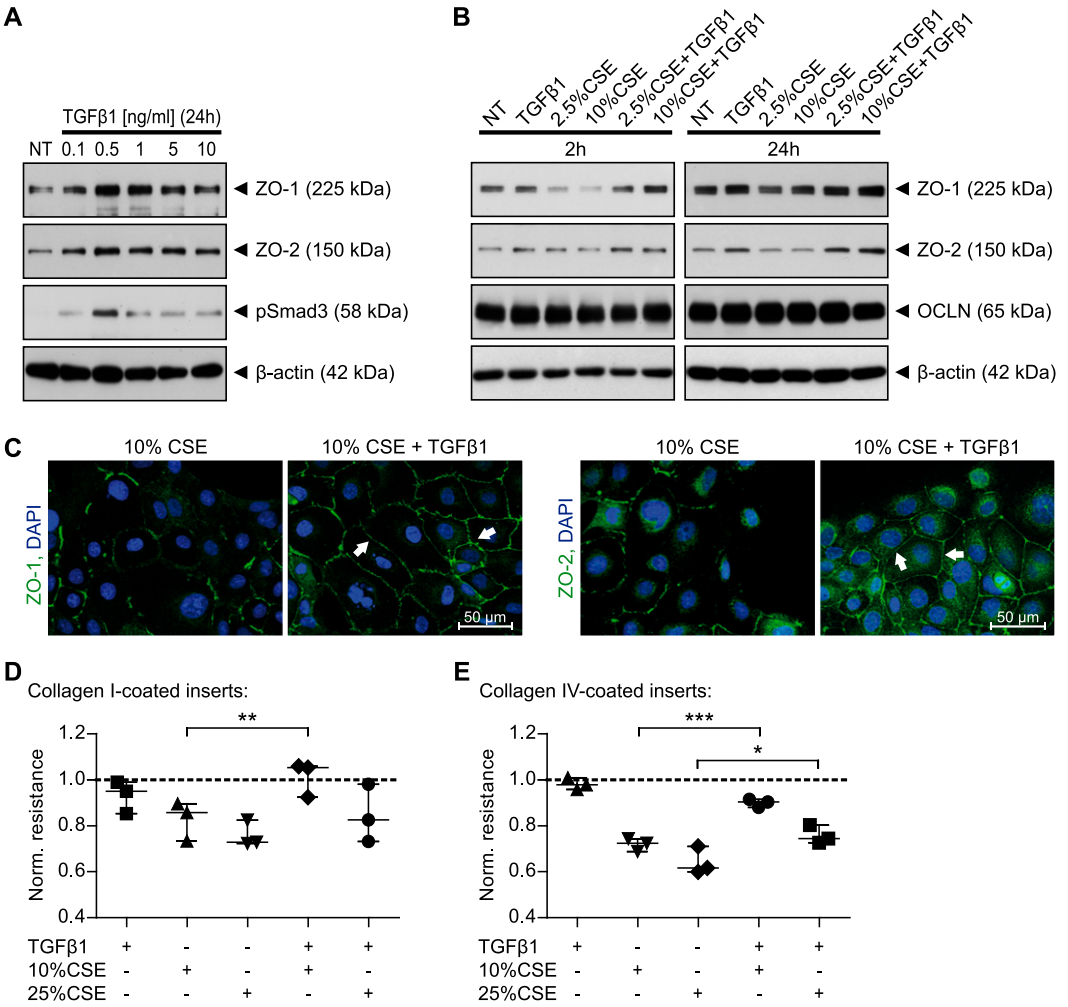

Figure 4. Short-term exposure of 16HBE14o$^-$ cells to transforming growth factor (TGF)-β1 prevents CSE-induced down-regulation of ZO-1 and ZO-2. (*A*) Western blot analysis of protein extracts from 16HBE14o$^-$ NT cells or cells treated with TGF-β1 (0.1–10 ng/ml) for 24 hours. Representative blots of tight junction proteins with corresponding β-actin as a loading control are shown. Phosphorylated Smad3 (pSmad3) served as a marker for the TGF-β1 response. (*B*) Western blot analysis of protein extracts from 16HBE14o$^-$ NT cells or cells treated with TGF-β1 (5 ng/ml), 2.5% CSE, 10% CSE alone or in combination for 2 and 24 hours. Representative blots of different tight junction proteins with corresponding β-actin as a loading control are shown. (*C*) Indirect immunofluorescence analysis of 16HBE14o$^-$ cells treated with 10% CSE or 10% CSE + TGF-β1 (5 ng/ml) for 72 hours (treatment every 24 h). Representative ZO-1 and ZO-2 staining is shown in *green*, and DAPI staining is shown in *blue*. *Scale bar*: 50 μm. *White arrows* indicate preserved tight junctions between the cells on TGF-β1 exposure. (*D*, *E*) Analysis of TEER from 16HBE14o$^-$ cells (cultured on collagen type I [*D*] or collagen type IV [*E*]) after exposure to TGF-β1 (5 ng/ml), 10% CSE, or 25% CSE alone or in combination for 6 hours. Data were normalized to pretreatment TEER values and untreated control. Data of three independent experiments with median ± quartile are shown. For all experiments, $^*P < 0.05$, $^{**}P < 0.01$, and $^{***}P < 0.001$ (Student's *t* test).

integrity is impaired by CSE via down-regulation of tight junction components, particularly by loss of ZO proteins from the membrane.

CSE Decreases ZO-1 Levels in Mouse Airways

To assess whether these *in vitro* effects were also observed in controlled exposures of intact bronchi, we performed an *ex vivo* analysis of mouse airways exposed to CSE. Mouse airways were incubated in control medium or in 5, 10, or 20% CSE for 2 hours under submerged conditions. Bronchi were transferred to ALI culture conditions in the presence of the same treatment media provided on the basal side. On exposure to CSE, ZO-1 transcript levels were significantly diminished in a time- and concentration-dependent manner (Figure 3A). In control airways, continuous apical staining of ZO-1 (red) between bronchial epithelial cells was observed by immunohistochemical analysis (Figure 3B), suggesting well-preserved tight junctions in control isolated airways. In contrast, we observed a striking difference in ZO-1 organization in CSE-exposed airways: ZO-1 staining was markedly reduced after CSE exposure for 24 hours, indicating disruption of junctional integrity. This finding was fully supportive of our *in vitro* results and indicated that CSE decreased tight junction components in bronchial epithelial cells *in vitro* and *ex vivo*.

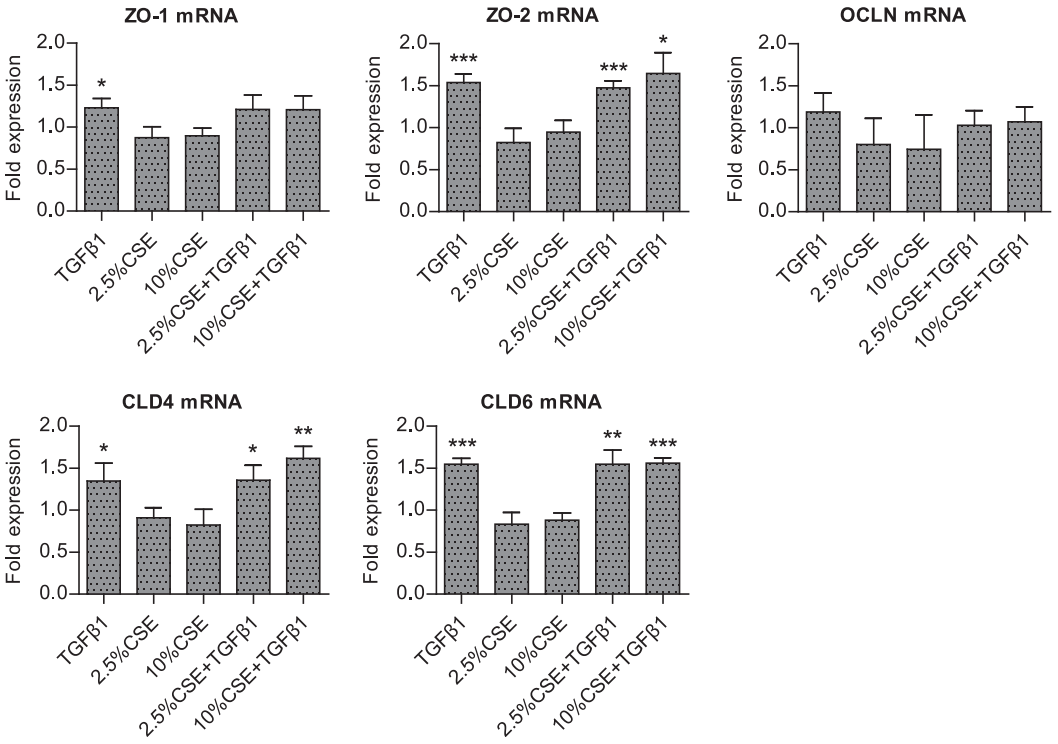

Figure 5. Long-term exposure of 16HBE14o$^-$ cells to TGF-β1 protects CSE-induced loss of tight junction components. Real-time quantitative reverse-transcriptase PCR analysis of expression levels of ZO-1, ZO-2, OCLN, CLD4, and CLD6 mRNA relative to controls. Cells were treated long term (every 24 h for seven times and split once in between) with TGF-β1 (5 ng/ml), 2.5% CSE, or 10% CSE alone or in combination. Values are depicted as mean ± SD of three independent experiments. *$P < 0.05$; **$P < 0.01$; ***$P < 0.001$ (Student's t test vs. controls).

TGF-β1 Counteracts CSE-Induced Barrier Dysfunction by Up-Regulation of Junctional Components

TGF-β has been reported to improve and decrease epithelial barrier function, depending on the organ and microenvironment investigated. We investigated the influence of TGF-β1 alone or in combination with CSE on bronchial epithelial cell junctional integrity. Cells were treated with TGF-β1 at the indicated concentrations for 24 hours, after which ZO-1 and ZO-2 protein levels were assessed by Western blot analysis (Figure 4A). All concentrations of TGF-β1 used increased ZO-1 and ZO-2 protein levels, with concomitant phosphorylation of Smad3 (pSmad3). Next, cells were treated for 2 and 24 hours with TGF-β1, CSE (2.5 and 10%), or a combination thereof (Figure 4B). After 2 hours, ZO-1 and ZO-2 protein levels were clearly down-regulated in CSE-treated cells compared with control (NT) cells (Figures 2 and 4B). Remarkably, TGF-β1 treatment protected bronchial epithelial cells from CSE-mediated down-regulation of tight junction proteins (Figure 4B). OCLN levels were not affected by TGF-β1 treatment. These findings were still evident 72 hours after treatment with 10% CSE or 10% CSE + TGF-β1, as demonstrated by immunofluorescence analysis (Figure 4C). Although membrane staining of ZO-1 and ZO-2 was disrupted by CSE treatment, addition of TGF-β1 prevented this effect and demonstrated continuous membrane staining of ZO-1 and ZO-2 at cell boundaries, mimicking the expression pattern of unstimulated cells.

To assess whether TGF-β1 is also able to functionally protect against CSE-induced barrier dysfunction, TEER of cells costimulated with CSE and TGF-β1 was measured (Figures 4D and 4E). Cells were plated on collagen I–coated (Figure 4D) or collagen IV–coated (Figure 4E) transwell inserts. Exposure to CSE clearly decreased TEER levels in both settings, whereas TGF-β1 alone did not change TEER levels compared with control. TGF-β1 cotreatment protected bronchial epithelial cells from CSE-induced barrier dysfunction. This effect was even more evident when cells were plated on collagen IV. To investigate whether TGF-β1 exerted its protective effect by increasing proliferation or cell survival, BrdU incorporation assay and PI/Annexin-V staining were performed, respectively (Figure E3). Cells treated for 24 and 72 hours with 10% CSE + TGF-β1 demonstrated a slight decrease in proliferation compared with CSE-treated cells (Figure E3A). TGF-β1 treatment did not affect apoptosis/necrosis ratios of the cells (Figure E3B).

We did not identify any changes in transcript levels of tight junction components within 24 hours of treatment with TGF-β1 or TGF-β1 combined with CSE (Figure E2). To analyze whether TGF-β1 affects transcriptional regulation of tight junction proteins after chronic exposure with CSE, cells were chronically treated, and RNA levels were analyzed by real-time quantitative reverse-transcriptase PCR (treatment scheme is pictured in Figure E4A). To control for effective responses of bronchial epithelial cells to TGF-β1, the expression of two TGF-β1 target genes, fibronectin and SNAIL, was analyzed. Both markers were markedly elevated by TGF-β1 and by TGF-β1 in combination with

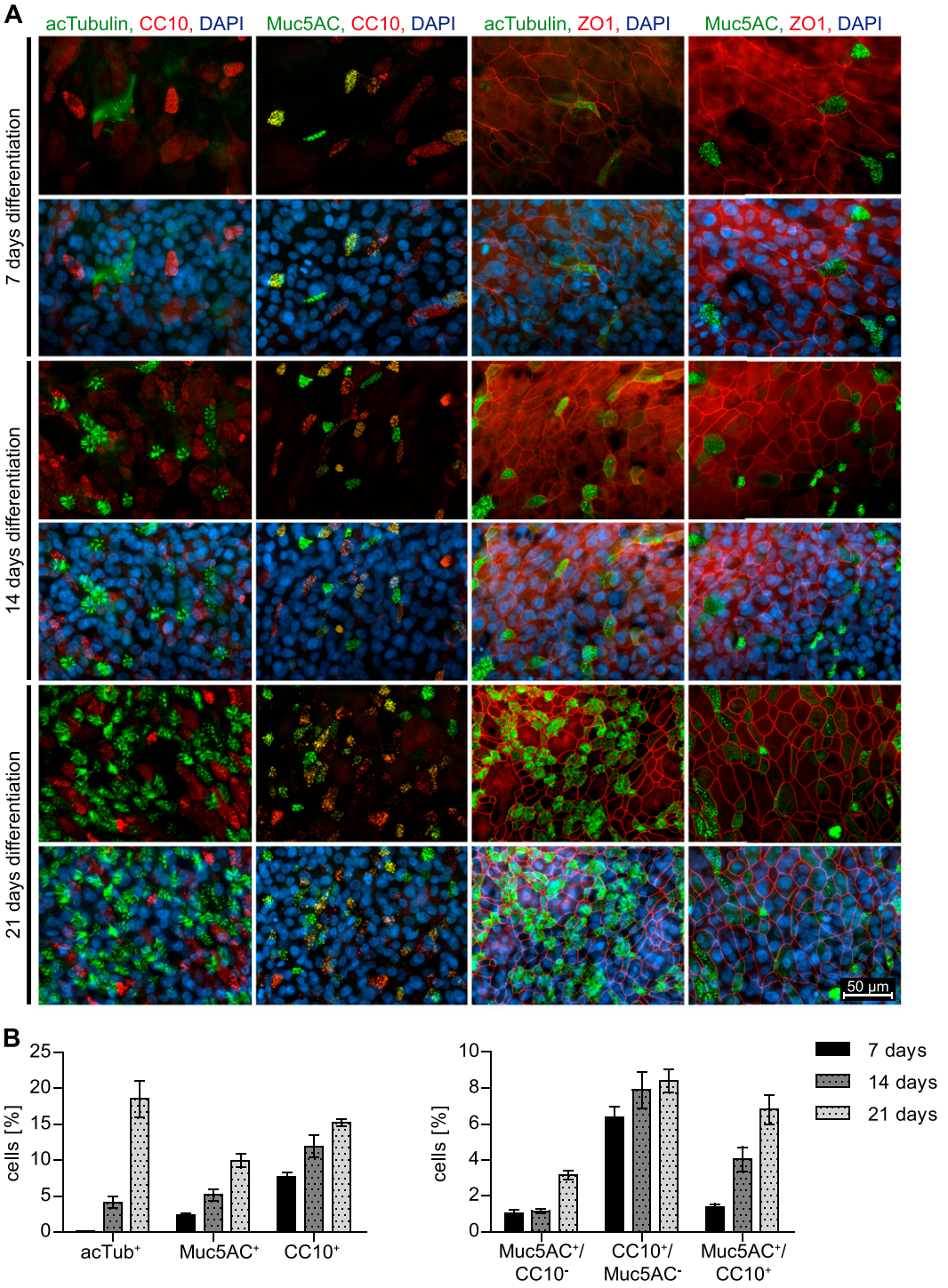

Figure 6. Primary human bronchial epithelial cells (pHBECs) at the air–liquid interface differentiate into a mucociliary epithelium. (*A*) Indirect immunofluorescence analysis of 7-, 14-, and 21-day differentiated pHBECs. Representative acetylated tubulin (acTubulin), CC10 (club cell [Clara cell]-specific 10 kDa protein), Muc5AC (mucin 5A/C), and ZO-1 staining is shown in *green* or *red*, and DAPI staining is shown in *blue*. *Scale bar*: 50 μm. (*B*) Data are depicted as mean ± SEM of independent differentiations relative to total number of cells. Ten images per group were analyzed.

CSE (Figure E4B). Next, we investigated how the expression of different junctional components is affected by TGF-β1 treatment (Figure 5). Of note, TGF-β1 induced up-regulation of several junctional proteins, such as ZO-1, ZO-2, CLD4, and CLD6, by up to 1.5-fold, with OCLN and E-cadherin (Figure E4B) transcript following the same trend. When cells were treated with a combination of TGF-β1 and CSE, similar effects could be observed: ZO-2, CLD4, and CLD6 mRNA levels were

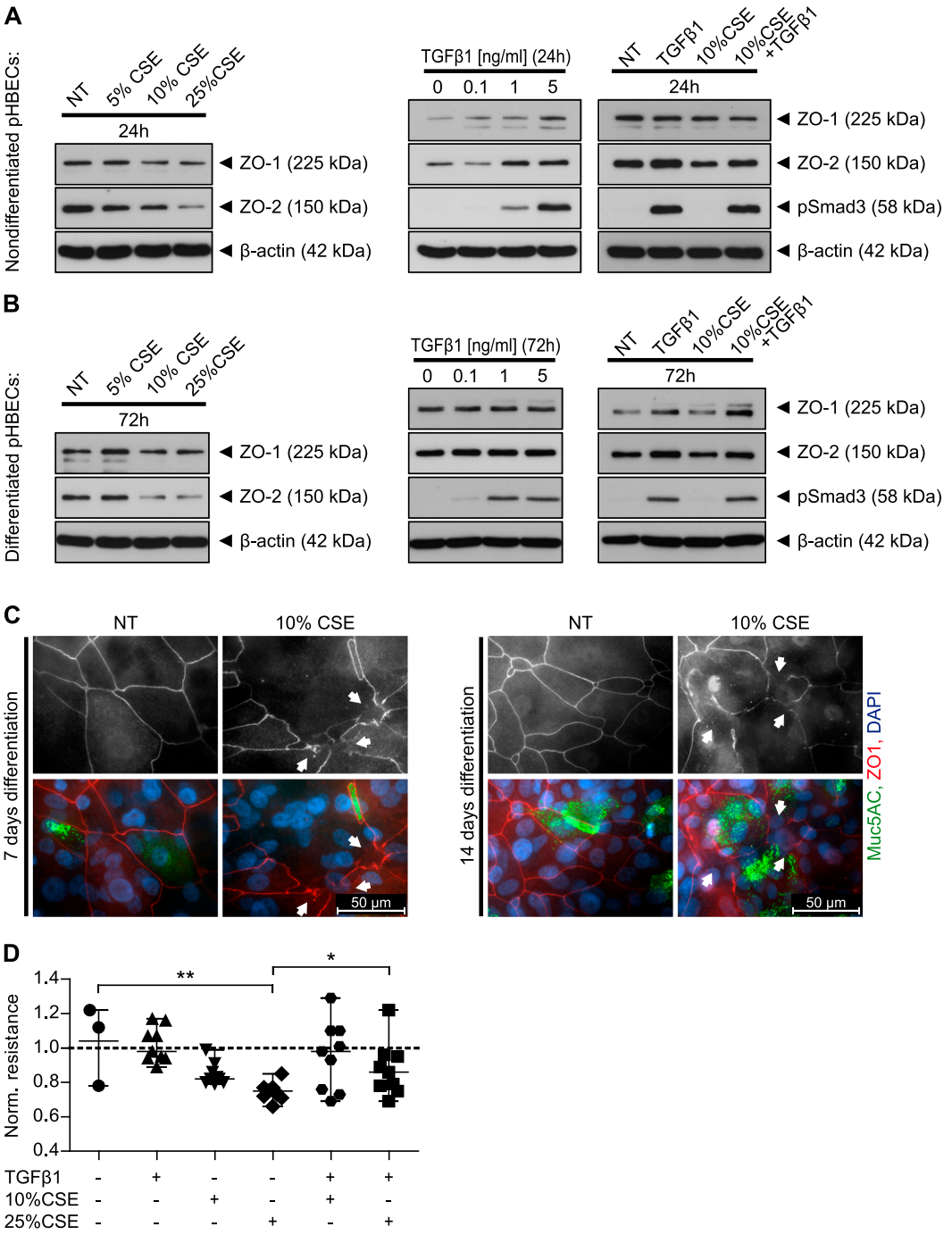

Figure 7. TGF-β1 exerts protective effects in pHBECs exposed to CSE. (*A*) Western blot analysis of protein extracts from nondifferentiated NT pHBECs or pHBECs treated for 24 hours with CSE (5–25%) (*left panel*), with TGF-β1 (0.1–5 ng/ml) (*middle panel*), or with 10% CSE, TGF-β1 (5 ng/ml), or 10% CSE + TGF-β1 (5 ng/ml) (*right panel*). Representative blots of ZO-1, ZO-2, and pSmad3 with representative β-actin as a loading control are shown. (*B*) Western blot analysis of protein extracts from differentiated NT pHBECs or pHBECs treated for 72 hours with CSE (5– 25%) (*left panel*), with TGF-β1 (0.1–5 ng/ml) (*middle panel*), or with 10% CSE, TGF-β1 (5 ng/ml), or 10% CSE + TGF-β1 (5 ng/ml) (*right panel*). Representative blots of ZO-1, ZO-2, and pSmad3 with representative β-actin as a loading control are shown. (*C*) Indirect immunofluorescence analysis of 7-day (*left panel*) or 14-day (*right panel*) differentiated pHBECs exposed to 10% CSE for 72 hours (treatment every 24 h). Representative ZO-1 staining is shown in *red*, Muc5AC staining is shown in *green*, and DAPI staining is shown in *blue*. *Scale bar*: 50 μm. *White arrows* indicate disrupted or zipper-like junctions between the cells on CSE exposure. (*D*) Analysis of TEER from differentiated pHBECs after exposure to TGF-β1 (5 ng/ml), 10% CSE, or 25% CSE alone or in combination for 6 hours. Data were normalized to pretreatment TEER values. Data of independent pHBEC differentiations with median ± quartile are shown. $^{*}P < 0.05$ and $^{**}P < 0.01$ (Student's *t* test).

significantly augmented in cells treated with TGF-β1 and CSE. ZO-1 and OCLN mRNA levels followed the same trend.

TGF-β1 Exerts its Protective Effect in CSE-Treated Differentiated Primary HBECs

To assess whether TGF-β1 can counteract CSE-induced barrier dysfunction in primary HBECs (pHBECs), we investigated two different settings: pHBECs were cultured on plastic (nondifferentiated) or at the ALI to achieve mucociliary differentiation. Effective differentiation was confirmed by immunofluorescence staining (Figure 6A) and quantification of differentiation makers (Figure 6B) over time. ZO-1 expression was present 7 days after air-lift and increased until 21 days. Acetylated-tubulin (ciliated cells), club cell (Clara cell)-specific 10 kDa protein (club cells), and Mucin 5AC (goblet cells) were expressed only on the apical side (Figure E6) and increased markedly over time. We also found some cells stained double positive for Muc5AC and CC10 after 21 days of differentiation (8.6%), whereas no cells were double positive for acetylated-tubulin and CC10. Basal cells that were positive for p63 were only found in the most basal cell layer (Figure E6).

To identify nontoxic doses of CSE, pHBECs were treated with a range of CSE concentrations for up to 72 hours, and lactate dehydrogenase assay was performed (Figure E5A). Up to 10% CSE did not trigger lactate dehydrogenase release from the cells, whereas 25% CSE was toxic in prolonged treatment for nondifferentiated cells. Differentiated pHBECs proved to be even more resistant to 25% CSE (Figure E5B). Next, we investigated whether CSE had similar effects on ZO-1 and ZO-2 expression levels in pHBECs, as observed with 16HBE14o$^-$ cells. After 24 hours of CSE exposure, we observed decreased ZO-1 and ZO-2 levels in a concentration-dependent manner (Figure 7A). ZO-1 and ZO-2 protein levels of differentiated cultures were clearly diminished after 72 hours of CSE exposure (Figure 7B). This might indicate higher resistance of differentiated cells to CSE injury. Moreover, differentiated pHBECs stimulated with 10% CSE for 72 hours demonstrated disrupted and/or zipper-like junctional appearance compared with control cells (Figure 7C). This result was further corroborated by TEER decrease after 10 and 25% CSE (Figure 7D). To test whether TGF-β1 treatment increased the expression of tight junction proteins in pHBECs, cells were treated with a range of TGF-β1 concentrations, and ZO-1 and ZO-2 levels were analyzed by Western blot. pSmad3 served as a positive control for TGF-β1 response (Figure 7A). After 24 hours of treatment, ZO-1 and ZO-2 protein levels were increased in a concentration-dependent manner. No differences in ZO-1 and ZO-2 levels were observed in differentiated pHBECs when treated with different TGF-β1 concentrations (Figure 7B).

Finally, we were interested whether TGF-β1 had the capacity to prevent CSE-induced injury in pHBECs. TGF-β1 protected pHBECs from CSE-mediated down-regulation of ZO-2 protein (Figure 7A). These findings were also evident in differentiated pHBECs (Figure 7B) that were treated for 72 hours with TGF-β1, 10% CSE, or 10% CSE + TGF-β1. Although 10% CSE decreased ZO-1 and ZO-2 protein levels, addition of TGF-β1 prevented this effect. These results were functionally reflected in TEER measurements: costimulation with CSE and TGF-β1 for 6 hours had a clear protective effect on loss of resistance compared with CSE only (Figure 7D). In accordance with our previous results, the protective effect of TGF-β1 was also evident in differentiated pHBECs.

Discussion

The bronchial epithelium is responsible for preserving airway homeostasis in the lung. It possesses innate defense functions and acts as a barrier against inhaled particles or pathogens. Epithelial barrier function is maintained by adherens junctions and, most importantly, by intercellular tight junctions. Here, we show that acute CSE exposure impaired the barrier function of HBECs. We also provide evidence that tight junction components were specifically affected by smoke injury. In particular, ZO-1 was displaced from the membrane fraction, contributing to severe tight junction disintegrity. Disruption of tight junctions with a loss of tight junction proteins from the membrane was confirmed in an *ex vivo* mouse model. Finally, TGF-β was able to prevent CSE-induced disruption of tight junction in HBECs and to preserve their barrier function.

Although the cytotoxic effects of cigarette smoke and its *in vitro* surrogate CSE on bronchial epithelial cells are well established, the mechanisms of cigarette smoke–induced impairment of bronchial epithelial barrier function are less well understood. Here, we analyzed the effects of CSE on tight junctions *in vitro* using the HBEC line 16HBE14o$^-$, pHBECs, and *ex vivo* using cultures of isolated mouse airways. Although 100 and 50% CSE induced acute cell death of bronchial epithelial cells, 10% CSE exposure neither decreased cell viability over long time periods nor affected cell morphology. Differentiated pHBECs proved even more resistant to CSE compared with 16HBE14o$^-$ cells and nondifferentiated pHBECs. Resistance measurements of 16HBE14o$^-$ monolayers (TEER) revealed a dose-dependent impairment of barrier function within 6 hours of CSE exposure at CSE doses of 10 and 25%, consistent with previous reports (13, 15, 30). As such, the regulation of barrier function by cigarette smoke is a specific effect and is not simply due to toxic effects. Because intact barrier function strongly depends on intact tight junctions, we studied the effects of smoke on tight junction proteins with respect to RNA and protein expression and subcellular localization.

Tight junction components, such as OCLN, CLDs, or junctional adhesion molecules, are linked to the actin cytoskeleton by ZO proteins, thereby enabling these proteins to constitute major stabilizing factors of tight junctions. Accordingly, ZO proteins have been shown to be essential for tight junction formation (31). In the current study, we observed a pronounced and acute loss of membrane-associated ZO-1 after CSE exposure. Similarly, ZO-2 and OCLN protein amounts were significantly decreased after CSE treatment, whereas CLD-4 and CLD-6 showed delayed down-regulation. Thus, junctional integrity was disrupted by CSE exposure. pHBECs showed a very similar response to CSE injury. In nondifferentiated and differentiated cultures, we observed a striking down-regulation of ZO-1 and ZO-2 protein levels when exposed to CSE. In agreement with our results, Heijink and colleagues (13) described delocalization of tight junction proteins from the junctions *in vitro* after

4 hours of CSE exposure. This agrees with an earlier report from Petecchia and colleagues (32), where ZO-1 staining decreased in a time- and concentration-dependent manner in CSE-stimulated bronchial epithelial cells.

In an *ex vivo* mouse model, we could confirm that CSE exposure had the capacity to reduce ZO-1 in fully intact mouse airways. The discrepancy that RNA levels of junctional components were affected in the *ex vivo* model but not in the cell line could be explained by the existing microenvironment in the *ex vivo* model and the different origins of the cells. Our finding that a tight junction protein (ZO-1) is diminished in murine bronchi on exposure to CSE is novel and shows for the first time the direct effect of cigarette smoke on a tight junction component *ex vivo*.

It is tempting to speculate that reduced ZO-1 expression is the underlying mechanism for the smoke-induced barrier dysfunction also reported *in vivo* (6, 8, 9). This notion is supported by findings in ZO-1/ZO-2–depleted mammary epithelial cells, reporting an inability to form tight junctions and epithelial resistance, as measured by TEER (31). In contrast, knockout of ZO-1 resulted in delayed tight junction and barrier formation (33) because of a compensatory increase of ZO-2. The concerted decrease of ZO-1 and ZO-2, which we found in CSE-exposed cells, might have similar effects: neither protein is able to compensate for the other, resulting in tight junction disintegrity. The central role of ZO-1 proteins in tight junction stability is also reflected by the fact that ZO-1 proteins are key for initiation of tight junction formation. ZO-1 is known to first colocalize with cadherins in spot-like adherens junctions. These gradually fuse to form mature, belt-like junctions and recruit CLDs/OCLN for tight junction polymerization (33). As soon as tight junctions are separated from adherens junctions in well-polarized cells, ZO-1 is exclusively concentrated at tight junctions. This suggests that loss of ZO-1 and ZO-2 due to cigarette smoke leads to destabilization of the junctions because polymerization of newly synthesized CLD and OCLN is impaired. CLD or OCLN proteins that are already polymerized at tight junctions are probably not directly affected by the loss of ZO proteins. This is indicated by the observation that protein levels of CLDs and OCLN remained unchanged and localized normally to the tight junctions in ZO-1/ZO-2–depleted cells (31). Besides ZO-1, OCLN has been reported to play a central role in tight junction stability and barrier function (34). Thus, its defect by cigarette smoke is most likely directly coupled to the resistance decrease found after cigarette smoke exposure.

Down-regulation of ZO-1 in bronchial epithelial cells was observed after 2 hours of CSE exposure and was still evident after 72 hours, as observed by membrane fractionation and immunofluorescence staining. Because RNA levels were not affected, these data strongly point toward an acute and posttranslational regulation of membrane-associated ZO-1 proteins by cigarette smoke, such as membrane distraction and degradation. Heijink and colleagues suggested that tight junction proteins are cleaved by calpains and lost from the membrane in response to cigarette smoke (13). For other membrane-bound proteins, such as the epidermal growth factor (EGF)-, vascular endothelial growth factor–, and IFN-γ receptor, it has been shown that cigarette smoke oxidatively modified these proteins, thereby priming them for membrane distraction and degradation by the ubiquitin proteasome system (35–38). There may be different reasons for the delayed down-regulation of CLDs by CSE that we have observed. First, CLDs have a much longer half-life than OCLN (39), which may protect these from CSE-dependent degradation as long as they are integrated within the junctional complex. Second, there is possibility that the CSE-dependent degradation of CLDs follows a different time course through different proteolytic pathways than the degradation of ZO-1, ZO-2, and OCLN and is therefore delayed.

TGF-β is known to play important roles in chronic lung disease. It is unclear if this multifunctional cytokine is protective or supportive to the pathogenesis of COPD. Herein, we found clear evidence that TGF-β1 protects from the disrupting effect of CSE on tight junctions. ZO-1 and ZO-2 were protected from membrane loss on exposure to CSE when bronchial epithelial cells were cotreated with TGF-β1. Only 2 hours of TGF-β1 stimulation prevented CSE-induced loss of tight junction proteins, and 24 hours of combined treatment with CSE and TGF-β1 enhanced protein levels of ZO-1 and ZO-2 compared with controls. This effect was specific for ZO-1 and ZO-2 because OCLN levels were not markedly enhanced on TGF-β1 stimulation. Furthermore, junctional integrity could be maintained in bronchial cells when cotreated with both CSE and TGF-β1, as indicated by the belt-like ZO-1 and ZO-2 immunofluorescence staining pattern resembling the localization of intact junctions of untreated cells. In addition, pHBECs exhibited a very similar response to TGF-β1 stimulation. In nondifferentiated and differentiated cultures, TGF-β1 prevented down-regulation of ZO-2 protein levels when cotreated with CSE. We also provide functional evidence that TGF-β1 prevented CSE-dependent loss of barrier function (TEER) in a dose-dependent manner. In line with our study, TGF-β has been shown to enhance epithelial barrier function in intestinal cells and to rescue barrier disruption caused by *Cryptosporidium parvum*, IFN-γ, or Enterohemorrhagic *Escherichia coli* O157:H7 (21–25). Besides TGF-β, EGF has been associated with tight junction protection in injured intestinal cells (40). This concept of barrier protection via EGF has recently been transferred to the lung field: EGF receptor positively regulates permeability barrier development through the Rac1/JNK-dependent pathway (41). Moreover, EGF treatment restored tight junctions in epithelial cultures from subjects with asthma (42). Therefore, we can speculate on the mechanisms of the protective effect of TGF-β, which may explain how airway epithelial cells circumvent the deleterious effects of CSE on tight junction integrity: TGF-β1 is endogenously released on smoke exposure, possibly as a protective mechanism *in vivo* (19, 43), and increased TGF-β1 activity down-regulates proteasomal activity in lung A549 cells (44). Potentially, TGF-β1 therefore counteracts proteasomal degradation of tight junction components by the proteasome, a degradation pathway previously reported to control ZO-1 and ZO-2 levels during tight junction disintegration (45). The capability of TGF-β1 to diminish the down-regulation of ZO-1 and ZO-2 protein levels after only 2 hours can only be explained by posttranslational regulation because no changes on transcript levels were observed within 24 hours of TGF-β1

stimulation. Only E-cadherin mRNA levels were found to be significantly increased within 24 hours of TGF-β1 stimulation. Because colocalization of ZO proteins with cadherins are key for tight junction formation (33) and because E-cadherin expression is crucial for proper tight junction architecture and epithelial resistance (46, 47), up-regulation of E-cadherin by TGF-β1 might help to stabilize tight junctions after CSE exposure. Up-regulation of ZO-1, ZO-2, CLD-4, or CLD-6 mRNA levels could be observed at later time points when cells were stimulated with TGF-β1 in combination with CSE. This strengthens the hypothesis that TGF-β1 not only protects but also counter-regulates the loss of tight junction proteins after injury.

Taken together, our results show that CSE disrupted tight junction integrity in HBECs. Similar results have been observed using an *ex vivo* mouse model. TGF-β1 prevented CSE-induced tight junction disruption and loss of barrier function. Because our data resemble molecular processes that largely occur after acute exposure to CSE, we speculate that protective spatiotemporal effects of TGF-β on the bronchial epithelium may play an important role in maintaining epithelial cell homeostasis, possibly preventing pathological remodeling in diseases such as COPD. ■

Author disclosures are available with the text of this article at www.atsjournals.org.

Acknowledgments: The authors thank Ann-Christin Beitel and Daniela Dietel for excellent technical assistance and Dr. Otmar Schmid (iLBD) for valuable discussion. They also thank D.C. Gruenert (University of California, San Francisco, CA) for providing the 16HBE14o- cells.

References

1. WHO. World health statistics 2008 (accessed 2012 Sept 11). Available from: http://www.who.int/whosis/whostat/EN_WHS08_Full.pdf
2. Decramer M, Janssens W, Miravitlles M. Chronic obstructive pulmonary disease. *Lancet* 2012;379:1341–1351.
3. Global Initiative for Chronic Obstructive Lung Disease. Global strategy for the diagnosis, management, and prevention of COPD. (updated 2010; accessed 2012 Sept 12). Available from: http://www.goldcopd.org/uploads/users/files/GOLDReport_April112011.pdf
4. Li XY, Rahman I, Donaldson K, MacNee W. Mechanisms of cigarette smoke induced increased airspace permeability. *Thorax* 1996;51:465–471.
5. Rusznak C, Mills PR, Devalia JL, Sapsford RJ, Davies RJ, Lozewicz S. Effect of cigarette smoke on the permeability and IL-1beta and sICAM-1 release from cultured human bronchial epithelial cells of never-smokers, smokers, and patients with chronic obstructive pulmonary disease. *Am J Respir Cell Mol Biol* 2000;23:530–536.
6. Jones JG, Minty BD, Lawler P, Hulands G, Crawley JC, Veall N. Increased alveolar epithelial permeability in cigarette smokers. *Lancet* 1980;1:66–68.
7. Burns AR, Hosford SP, Dunn LA, Walker DC, Hogg JC. Respiratory epithelial permeability after cigarette smoke exposure in guinea pigs. *J Appl Physiol (1985)* 1989;66:2109–2116.
8. Simani AS, Inoue S, Hogg JC. Penetration of the respiratory epithelium of guinea pigs following exposure to cigarette smoke. *Lab Invest* 1974;31:75–81.
9. Hulbert WC, Walker DC, Jackson A, Hogg JC. Airway permeability to horseradish peroxidase in guinea pigs: the repair phase after injury by cigarette smoke. *Am Rev Respir Dis* 1981;123:320–326.
10. Guillemot L, Paschoud S, Pulimeno P, Foglia A, Citi S. The cytoplasmic plaque of tight junctions: a scaffolding and signalling center. *Biochim Biophys Acta* 2008;1778:601–613.
11. González-Mariscal L, Betanzos A, Nava P, Jaramillo BE. Tight junction proteins. *Prog Biophys Mol Biol* 2003;81:1–44.
12. Baum SL, Andreson IGM, Baker RR, Murphy DM, Rowlands CC. Electron spin resonance and spin trap investigation of free radicals in cigarette smoke: development of a quantification procedure. *Anal Chim Acta* 2003;481:1–13.
13. Heijink IH, Brandenburg SM, Postma DS, van Oosterhout AJ. Cigarette smoke impairs airway epithelial barrier function and cell-cell contact recovery. *Eur Respir J* 2012;39:419–428.
14. Olivera DS, Boggs SE, Beenhouwer C, Aden J, Knall C. Cellular mechanisms of mainstream cigarette smoke-induced lung epithelial tight junction permeability changes in vitro. *Inhal Toxicol* 2007;19:13–22.
15. Shaykhiev R, Otaki F, Bonsu P, Dang DT, Teater M, Strulovici-Barel Y, Salit J, Harvey BG, Crystal RG. Cigarette smoking reprograms apical junctional complex molecular architecture in the human airway epithelium in vivo. *Cell Mol Life Sci* 2011;68:877–892.
16. Veljkovic E, Jiricny J, Menigatti M, Rehrauer H, Han W. Chronic exposure to cigarette smoke condensate in vitro induces epithelial to mesenchymal transition-like changes in human bronchial epithelial cells, BEAS-2B. *Toxicol In Vitro* 2011;25:446–453.
17. Coker RK, Laurent GJ, Shahzeidi S, Hernández-Rodríguez NA, Pantelidis P, du Bois RM, Jeffery PK, McAnulty RJ. Diverse cellular TGF-beta 1 and TGF-beta 3 gene expression in normal human and murine lung. *Eur Respir J* 1996;9:2501–2507.
18. Hogg JC, Timens W. The pathology of chronic obstructive pulmonary disease. *Annu Rev Pathol* 2009;4:435–459.
19. de Boer WI, van Schadewijk A, Sont JK, Sharma HS, Stolk J, Hiemstra PS, van Krieken JH. Transforming growth factor beta1 and recruitment of macrophages and mast cells in airways in chronic obstructive pulmonary disease. *Am J Respir Crit Care Med* 1998;158:1951–1957.
20. Wu L, Chau J, Young RP, Pokorny V, Mills GD, Hopkins R, McLean L, Black PN. Transforming growth factor-beta1 genotype and susceptibility to chronic obstructive pulmonary disease. *Thorax* 2004;59:126–129.
21. Planchon SM, Martins CA, Guerrant RL, Roche JK. Regulation of intestinal epithelial barrier function by TGF-beta 1: evidence for its role in abrogating the effect of a T cell cytokine. *J Immunol* 1994;153:5730–5739.
22. Roche JK, Martins CA, Cosme R, Fayer R, Guerrant RL. Transforming growth factor beta1 ameliorates intestinal epithelial barrier disruption by Cryptosporidium parvum in vitro in the absence of mucosal T lymphocytes. *Infect Immun* 2000;68:5635–5644.
23. Planchon S, Fiocchi C, Takafuji V, Roche JK. Transforming growth factor-beta1 preserves epithelial barrier function: identification of receptors, biochemical intermediates, and cytokine antagonists. *J Cell Physiol* 1999;181:55–66.
24. McKay DM, Singh PK. Superantigen activation of immune cells evokes epithelial (T84) transport and barrier abnormalities via IFN-gamma and TNF alpha: inhibition of increased permeability, but not diminished secretory responses by TGF-beta2. *J Immunol* 1997;159:2382–2390.
25. Howe KL, Reardon C, Wang A, Nazli A, McKay DM. Transforming growth factor-beta regulation of epithelial tight junction proteins enhances barrier function and blocks enterohemorrhagic *Escherichia coli* O157:H7-induced increased permeability. *Am J Pathol* 2005;167:1587–1597.
26. van Rijt SH, Keller IE, John G, Kohse K, Yildirim AO, Eickelberg O, Meiners S. Acute cigarette smoke exposure impairs proteasome function in the lung. *Am J Physiol Lung Cell Mol Physiol* 2012;303:L814–L823.
27. Yildirim AO, Veith M, Rausch T, Müller B, Kilb P, Van Winkle LS, Fehrenbach H. Keratinocyte growth factor protects against Clara cell injury induced by naphthalene. *Eur Respir J* 2008;32:694–704.

28. Mise N, Savai R, Yu H, Schwarz J, Kaminski N, Eickelberg O. Zyxin is a transforming growth factor-β (TGF-β)/Smad3 target gene that regulates lung cancer cell motility via integrin α5β1. *J Biol Chem* 2012;287:31393–31405.
29. Kneidinger N, Yildirim AO, Callegari J, Takenaka S, Stein MM, Dumitrascu R, Bohla A, Bracke KR, Morty RE, Brusselle GG, *et al*. Activation of the WNT/β-catenin pathway attenuates experimental emphysema. *Am J Respir Crit Care Med* 2011;183:723–733.
30. Gangl K, Reininger R, Bernhard D, Campana R, Pree I, Reisinger J, Kneidinger M, Kundi M, Dolznig H, Thurnher D, *et al*. Cigarette smoke facilitates allergen penetration across respiratory epithelium. *Allergy* 2009;64:398–405.
31. Umeda K, Ikenouchi J, Katahira-Tayama S, Furuse K, Sasaki H, Nakayama M, Matsui T, Tsukita S, Furuse M, Tsukita S. ZO-1 and ZO-2 independently determine where claudins are polymerized in tight-junction strand formation. *Cell* 2006;126:741–754.
32. Petecchia L, Sabatini F, Varesio L, Camoirano A, Usai C, Pezzolo A, Rossi GA. Bronchial airway epithelial cell damage following exposure to cigarette smoke includes disassembly of tight junction components mediated by the extracellular signal-regulated kinase 1/2 pathway. *Chest* 2009;135:1502–1512.
33. Umeda K, Matsui T, Nakayama M, Furuse K, Sasaki H, Furuse M, Tsukita S. Establishment and characterization of cultured epithelial cells lacking expression of ZO-1. *J Biol Chem* 2004;279: 44785–44794.
34. Cummins PM. Occludin: one protein, many forms. *Mol Cell Biol* 2012; 32:242–250.
35. Meiners S, Eickelberg O. What shall we do with the damaged proteins in lung disease? Ask the proteasome! *Eur Respir J* 2012;40: 1260–1268.
36. Dorofeyeva LV. Obtaining of measles virus haemagglutinin from strain L-16 grown in primary cell cultures. *Acta Virol* 1975;19:497.
37. HuangFu WC, Liu J, Harty RN, Fuchs SY. Cigarette smoking products suppress anti-viral effects of type i interferon via phosphorylation-dependent downregulation of its receptor. *FEBS Lett* 2008;582: 3206–3210.
38. Khan EM, Lanir R, Danielson AR, Goldkorn T. Epidermal growth factor receptor exposed to cigarette smoke is aberrantly activated and undergoes perinuclear trafficking. *FASEB J* 2008;22:910–917.
39. Traweger A, Fang D, Liu YC, Stelzhammer W, Krizbai IA, Fresser F, Bauer HC, Bauer H. The tight junction-specific protein occludin is a functional target of the E3 ubiquitin-protein ligase itch. *J Biol Chem* 2002;277:10201–10208.
40. Samak G, Aggarwal S, Rao RK. ERK is involved in EGF-mediated protection of tight junctions, but not adherens junctions, in acetaldehyde-treated Caco-2 cell monolayers. *Am J Physiol Gastrointest Liver Physiol* 2011;301:G50–G59.
41. Terakado M, Gon Y, Sekiyama A, Takeshita I, Kozu Y, Matsumoto K, Takahashi N, Hashimoto S. The Rac1/JNK pathway is critical for EGFR-dependent barrier formation in human airway epithelial cells. *Am J Physiol Lung Cell Mol Physiol* 2011;300:L56–L63.
42. Xiao C, Puddicombe SM, Field S, Haywood J, Broughton-Head V, Puxeddu I, Haitchi HM, Vernon-Wilson E, Sammut D, Bedke N, *et al*. Defective epithelial barrier function in asthma. *J Allergy Clin Immunol* 2011;128:549–556, e1–e12.
43. Takizawa H, Tanaka M, Takami K, Ohtoshi T, Ito K, Satoh M, Okada Y, Yamasawa F, Nakahara K, Umeda A. Increased expression of transforming growth factor-beta1 in small airway epithelium from tobacco smokers and patients with chronic obstructive pulmonary disease (COPD). *Am J Respir Crit Care Med* 2001;163: 1476–1483.
44. Ali A, Wang Z, Fu J, Ji L, Liu J, Li L, Wang H, Chen J, Caulin C, Myers JN, *et al*. Differential regulation of the REGγ-proteasome pathway by p53/TGF-β signalling and mutant p53 in cancer cells. *Nat Commun* 2013;4:2667.
45. Nakamuta S, Endo H, Higashi Y, Kousaka A, Yamada H, Yano M, Kido H. Human immunodeficiency virus type 1 gp120-mediated disruption of tight junction proteins by induction of proteasome-mediated degradation of zonula occludens-1 and -2 in human brain microvascular endothelial cells. *J Neurovirol* 2008;14: 186–195.
46. Heijink IH, Brandenburg SM, Noordhoek JA, Postma DS, Slebos DJ, van Oosterhout AJ. Characterisation of cell adhesion in airway epithelial cell types using electric cell-substrate impedance sensing. *Eur Respir J* 2010;35:894–903.
47. Tunggal JA, Helfrich I, Schmitz A, Schwarz H, Günzel D, Fromm M, Kemler R, Krieg T, Niessen CM. E-cadherin is essential for in vivo epidermal barrier function by regulating tight junctions. *EMBO J* 2005;24:1146–1156.